Polymer 53 (2012) 1288–1297

Contents lists available at SciVerse ScienceDirect

Polymer

journal homepage: www.elsevier.com/locate/polymer

Synthesis and characterization of novel polyampholyte and polyelectrolyte polymers containing imidazole, triazole or pyrazole

Juan M. Lázaro Martínez [a,b], Ana K. Chattah [b], Rosa M. Torres Sánchez [c], Graciela Y. Buldain [a,*], Viviana Campo Dall' Orto [d,**]

[a] Departamento de Química Orgánica, Facultad de Farmacia y Bioquímica, Universidad de Buenos Aires, Junín 956 (C1113AAD), Ciudad Autónoma de Buenos Aires, Argentina
[b] Facultad de Matemática, Astronomía y Física, Universidad Nacional de Córdoba, IFEG-CONICET, (5000) Córdoba, Argentina
[c] Centro de Tecnología de Recursos Minerales y Cerámica (CETMIC), Camino Centenario y 506, (1897) Gonnet, Argentina
[d] Departamento de Química Analítica y Fisicoquímica, Facultad de Farmacia y Bioquímica, Universidad de Buenos Aires, Junín 956 (C1113AAD), Ciudad Autónoma de Buenos Aires, Argentina

ARTICLE INFO

Article history:
Received 15 December 2011
Accepted 19 January 2012
Available online 25 January 2012

Keywords:
Non-soluble materials
Ionic polymers
Solid-state NMR

ABSTRACT

Novel soluble and non-soluble polymers based on methacrylic acid, ethylene glycol diglycidyl ether and pyrazole, triazole or imidazole were obtained by a one-spot synthetic strategy. The new materials were characterized by spectroscopic techniques (FT-IR, and solution- and solid-state NMR). Evidence on the covalent binding of the different heterocycles to the non-soluble matrix was given by the unequivocal assignment of the ^{13}C solid-state NMR spectra. Proton relaxation times in the rotating frame and two-dimensional wideline separation (^{1}H-^{13}C WISE) NMR spectra were used to assess their molecular dynamics. The higher synthetic yield of polyampholytes bearing triazole or pyrazole correlated with a lower molecular motion and a higher cross-linking degree. The polyelectrolyte effect of these materials was exhaustively explored through the acid-base properties, swelling and zeta potential. The quaternization of heterocyclic residues, responsible for adsorptive properties, was studied taking into account that these materials are attractive for analytical, environmental and biotechnological processes.

1. Introduction

Polymers containing ionic groups are among the most important classes of macromolecules. These materials may be divided into two groups: polyelectrolytes and polyzwitterions. Polyelectrolytes contain anionic or cationic groups, whereas polyzwitterions contain both anionic and cationic groups. The polyzwitterions that specifically possess the charged groups in different monomer units are named polyampholytes. There are four different subclasses of polyampholytes based on their responses to changes in pH, where the anionic and/or cationic groups may be neutralized and/or may be insensitive to changes in pH [1–4]. A characteristic of polyelectrolytes is chain expansion in deionized water due to Coulombic repulsions. The addition of low molecular weight electrolyte or changes in the solution pH screens the repulsive electrostatic forces, and the polymer coil shrinks. This is known as the polyelectrolyte effect [5]. Polyampholytes have the ability to demonstrate both polyelectrolyte and antipolyelectrolyte behavior depending on the composition of the solution in contact. Another characteristic feature of polyampholytes, in particular those composed of weak acid and base species, is that they possess an isoelectric point, defined as the pH at which the polyampholyte is electrically neutral.

Non-soluble ionic polymers find a huge variety of applications in analytical and synthetic fields in solid-phase development for ion-chromatography, protein separation, molecular imprinting, catalysis and chemical sensors [6–9]. In the same way, the development of polymers containing nitrogen as donor atoms is particularly strong due to the applications as destabilizing negative colloids in effluents and water clarification [10], recovery of trace metal ions [11], and biotechnology issues [12,13], among others [14]. Polyvinylimidazole is an example of great relevance because it is relatively simple to synthesize and can generate permanent positive charge densities by controlled quarternization [15].

In this work, we present the non-soluble polyampholytes *Poly*(EGDE-MAA-PYR) and *Poly*(EGDE-MAA-TRZ), together with the polyelectrolytes *Poly*(EGDE-IM) and *Poly*(EGDE-2MI) based on ethylene glycol diglycidyl ether (EGDE), methacrylic acid (MAA)

* Corresponding author. Tel./fax: +54 11 49648200x8351.
** Corresponding author. Tel./fax: +54 11 49648263.
E-mail addresses: gbuldain@ffyb.uba.ar (G.Y. Buldain), vcdall@ffyb.uba.ar (V. Campo Dall' Orto).

0032-3861/$ – see front matter © 2012 Elsevier Ltd. All rights reserved.
doi:10.1016/j.polymer.2012.01.031

and/or nitrogen-heterocycle monomers (IM = imidazole, 2MI = 2-methylimidazole, PYR = pyrazole, or TRZ = triazole) obtained by a one-spot synthetic strategy. The selection of these heterocycle units was based on the possibility of modulating the acid-base properties and the isoelectric point of the polymer matrices obtained, because it is a critical factor that should be taken into account when a material is used as a solid phase for extraction, for instance for protein uptake [16–18]. These kinds of materials have been proved to be efficient matrixes for ion and macromolecule adsorption with potential applications in environmental protection and analysis [19,20]. The new materials were characterized by spectroscopic techniques such as SEM, FT-IR and solid-state NMR. In addition, other NMR techniques such as wideline separation (^{1}H-^{13}C 2D-WISE) and proton relaxation times in the rotating frame ($T^H_{1\rho}$) were used to assess their molecular dynamics. The polyelectrolyte effect of these materials was exhaustively explored through the acid-base properties, swelling and zeta potential dependence on pH. The quaternization of imidazole, triazole or pyrazole residues, an important factor to characterize charged materials, was also studied.

2. Materials and methods

2.1. Polymer synthesis

The novel polyampholytes *Poly*(EGDE-MAA-TRZ) and *Poly*(EGDE-MAA-PYR) were synthesized with 1.0 mL of methacrylic acid (MAA) purified by vacuum distillation, 2.0 mL of ethylene glycol diglycidyl ether (EGDE; 50 wt% in ethylene glycol dimethyl ether) and the corresponding heterocycle (1.02 g of 1*H*-1,2,4-triazole = TRZ 98 wt% or 830 mg of pyrazole = PYR 98 wt%) were mixed with 10.0 mL of acetonitrile. After that, 30 mg of benzoyl peroxide was added to the reaction. The solutions were placed in a tube glass and thermostated at 60 °C for 24 h. The material was placed at 20 °C, milled in particles, washed three times with distilled water and dried. The elemental analysis for *Poly*(EGDE-MAA-TRZ) showed that: N, 7.7%; C, 49.5%; H, 7.4%; whereas that for *Poly*(EGDE-MAA-PYR) showed that: N, 5.5%; C, 53.8%; H, 7.6%.

The non-soluble polyelectrolytes *Poly*(EGDE-IM or 2MI) were synthesized in the same way, with EGDE (2.0 mL) and the corresponding functional monomer (820 mg of imidazole = IM 99 wt% or 1 g of 2-methylimidazole = 2MI 99 wt%) in 8.0 mL of acetonitrile. The solutions were placed in a tube glass and thermostated at 60 °C for 24 h. The material was placed at 20 °C, milled in particles, washed three times with distilled water and dried. The elemental analysis for *Poly*(EGDE-IM) showed that: N, 5.9%; C, 51.9%; H, 8.0%; whereas that for *Poly*(EGDE-2MI) showed that: N, 5.7%; C, 51.7%; H, 8.0%.

The soluble *Poly*(EGDE-IM)$_{sol}$ was synthesized with EGDE (1.0 mL) and imidazole (820 mg) in 8.0 mL of acetonitrile. The solution was placed in a tube glass and thermostated at 60 °C for 24 h. The material was placed at 20 °C, dissolved with 2.0 mL of distilled water, and the resulting solution then washed with chloroform (3 × 2.0 mL). Finally, the aqueous solution were lyophilized for 48 h and studied by solution-state NMR and high resolution ESI-MS experiments.

The polyampholytes *Poly*(EGDE-MAA-IM or 2MI) and the polyelectrolyte *Poly*(EGDE-MAA) were synthesized according to previous reports [20].

2.2. Experimental section

2.2.1. General

Elemental analysis was performed with a CE440 Exeter Analytical device. A nitrogen adsorption isotherm was collected at 77 K on a Micromeritics Gemini 2360 system. The adsorption of water was made in a hygrostat at 55% of relative humidity, the water content in the monolayer was determined by gravimetry, and the surface area of adsorption was calculated taking into account the surface area of a water molecule (10.6×10^{-20} m^2). Particle size determination (1% w/w water suspension) was performed by dynamic light scattering measurements using the Brookhaven 90Plus/Bi-MAS Multi Angle Particle Sizing, operating at λ = 635 nm, 35 mW-solid state laser, scattering angle 90°, 25 ± 0.1 °C. The determination only gives an apparent equivalent sphere diameter (D_{app}). FT-IR spectra were recorded on a Nicolet 360 spectrometer using KBr pellets. SEM images were carried out with a scanning electron microscope (Zeiss Gemini DSM 982) operated at a 0.3 kV acceleration voltage. The solution-state NMR experiments were performed on a Bruker Avance-II 500 MHz. The high resolution ESI-MS spectra were determined on a Bruker micrOTOF-Q II. Zeta (ζ) Potential measurements were performed with a Zeta Potential Analyzer ZetaPlus from Brokhaven Instruments Corporation at 25 °C and constant ionic strength of 10^{-3} M KCl. Potentiometric titrations of the solvated functional groups were carried out with a HANNA Instrument pH meter model HI8424 supplied with a combined glass electrode, according to previous reports [20]. Equilibrium swelling measurements were performed according to previous reports [20].

2.2.2. Solid-state NMR

High-resolution ^{13}C solid-state spectra for the polymers were recorded using the ramp {^{1}H}→{^{13}C} CP-MAS (cross-polarization and magic angle spinning) sequence with proton decoupling during acquisition. All the solid-state NMR experiments were performed at room temperature in a Bruker Avance II-300 spectrometer equipped with a 4-mm MAS probe. The operating frequency for protons and carbons was 300.13 and 75.46 MHz, respectively. Glycine was used as an external reference for the ^{13}C spectra and to set the Hartmann-Hahn matching condition in the cross-polarization experiments. The recycling time was 4 s. The contact time during CP was 1.5 ms for the polymer materials. The two-pulse phase modulation (TPPM) or the SPINAL64 sequences were used for heteronuclear decoupling during acquisition with a proton field H_{1H} satisfying $\omega_{1H}/2\pi = \gamma_H H_{1H}$ = 62 kHz [21,22]. The spinning rate for all the samples was 10 kHz.

Proton spin lattice relaxation time in the rotating frame, $T^H_{1\rho}$, was measured through carbon spectra at the proton spin-lock field: $\omega_{1H}/2\pi$ = 40 kHz. The variable time τ ranged from 10 μs to 7.5 ms. Contact time between carbon and protons was 100 μs, allowing the ^{13}C polarization to be dominated only by the ^{1}H directly bound to the carbons. The 2D ^{1}H-^{13}C WISE (wideline separation) experiment was performed following the pulse sequence developed by Schmidt-Rohr et al. at room temperature [23]. The proton magnetization was transferred to ^{13}C using a short CP contact time of 200 μs in order to avoid equilibration of the proton magnetization due to spin diffusion. The MAS frequency was set to 4.5 kHz in order not to affect the proton lineshape. In our experiment, 32 increments of 3 μs were

Table 1
Monomer composition, apparent diameter (D_{app}) and surface area of the particles for the different materials.

Polymer	Monomer			D_{app} (μm)	Surface area[b] ($m^2\ g^{-1}$)
	EGDE	MAA	HET[a]		
EGDE-2MI	0.83	–	0.17	59.2	260
EGDE-IM	0.70	–	0.30	65.4	243
EGDE-MAA-TRZ	0.41	0.46	0.13	30.1	274
EGDE-MAA-PYR	0.61	0.26	0.13	1.6	216
EGDE-MAA-IM	0.49	0.35	0.16	67.7	367
EGDE-MAA	0.35	0.65	–	35.1	83

[a] Heterocyclic ring depending on the polymer material.
[b] Surface areas obtained from water adsorption.

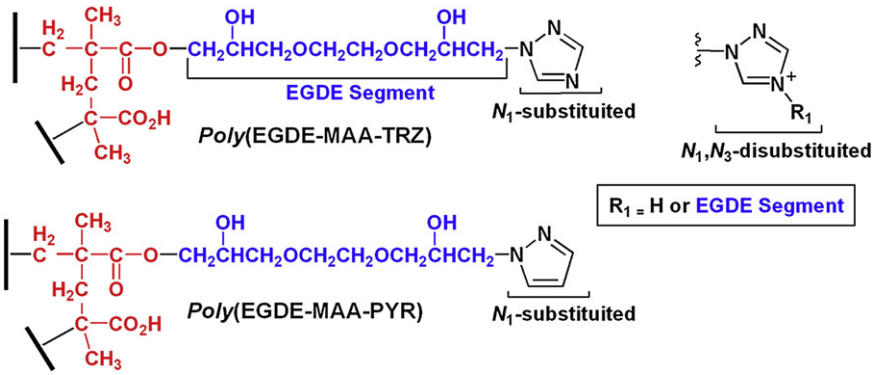

Scheme 1. Representative chemical structures of the novel polyampholytes.

collected in the indirect ^{1}H dimension. HETCOR spectrum in the solid state was recorded for *Poly*(EGDE-2MI) following the sequence presented by van Rossum et al. [24]. The contact time for the CP was 200 μs to avoid relayed homonuclear spin-diffusion-type processes. The magic angle pulse length was 2.55 μs. To obtain the ^{1}H spectra, 64 points were collected with a dwell time of 35.5 μs. The acquisition time was 1.14 ms and the spinning rate was 10 kHz.

3. Results and discussion

3.1. Synthesis and characterization of non-soluble ionic polymers, Poly(EGDE-MAA-TRZ), Poly(EGDE-MAA-PYR) and Poly(EGDE-2MI)

Although we have previously reported the synthesis and characterization of ionic polymers bearing imidazole units, the synthetic yield was affected by the ionic pair formed between the methacrylic acid (MAA) and the imidazole ring, which reduced the reactivity of the monomers [20]. The analysis of the pKa values for the MAA (pKa = 4.66) and the protonated species: imidazole (pKa = 7.18), pyrazole (pKa = 2.5) and triazole ring (pKa = 2.39) showed that only the imidazole derivatives had the disadvantage of the formation of the ionic pair between the mentioned monomers with MAA. In the new materials reported here, the yields were increased to 80-90% using pyrazole or triazole respectively. Table 1 shows the polymer composition for the different materials studied.

The novel non-soluble polyampholytes were synthesized in a one-step batch synthetic strategy using methacrylic acid (MAA), ethylene glycol diglycidyl ether (EGDE) and pyrazole (PYR) or triazole (TRZ) in the presence of benzoyl peroxide. Scheme 1 exhibits the most representative chemical structures of these products. Three parallel reactions take place in these polymer materials: radical polymerization of MAA, which gives linear segments, like *Poly*(MAA), condensation between EGDE and MAA monomers, and reaction of some epoxy-units with pyrazole or triazole, which results in N_1-substituted units. These N_1-substituted azole units may react with other oxirane ring to give rise to N_1,N_3-disubstituted triazole units or N_1,N_2-disubstituted pyrazole units. Furthermore, linear *Poly*(MAA) segments interact with azole moieties of the EGDE-PYR or EGDE-TRZ fragments, giving some kind of interpolymeric complex, which results in an interesting system with interpenetration of linear and cross-linked polymers.

Finally, the synthesis of *Poly*(EGDE-2MI or IM) was carried out to improve the NMR assignment of the ^{13}C CP-MAS spectra and for the zeta potential studies that are discussed below in the manuscript. In agreement with the kinetic results obtained by Barton [25] and Chiu et al. [26] for the curing of epoxy resins using different concentrations of imidazole, we postulated a possible mechanism of reaction (Scheme 2). Initially, the pyridine-type nitrogen of 2-methylimidazole (2MI) causes the opening of the epoxy group present in the EGDE molecule with the concomitant proton transfer and the generation of a new pyridine-type nitrogen, which subsequently reacts with a new EGDE molecule (Scheme 2, Step A), giving rise to a N_1,N_3-disubstituted 2MI unit and an alkoxide intermediate. The latter generates cross-linking between EGDE chains through a polyesterification mechanism (Scheme 2, Step B). In particular, the new polyelectrolyte materials, *Poly*(EGDE-IM or 2MI), were rendered as slack materials, indicative of a low cross-linking degree, with a yield of around 60-70%.

3.2. Surface and FTIR characterization

SEM images were obtained without surface modifications (Fig. 1). Particularly, the SEM image of *Poly*(EGDE-MAA-TRZ) was

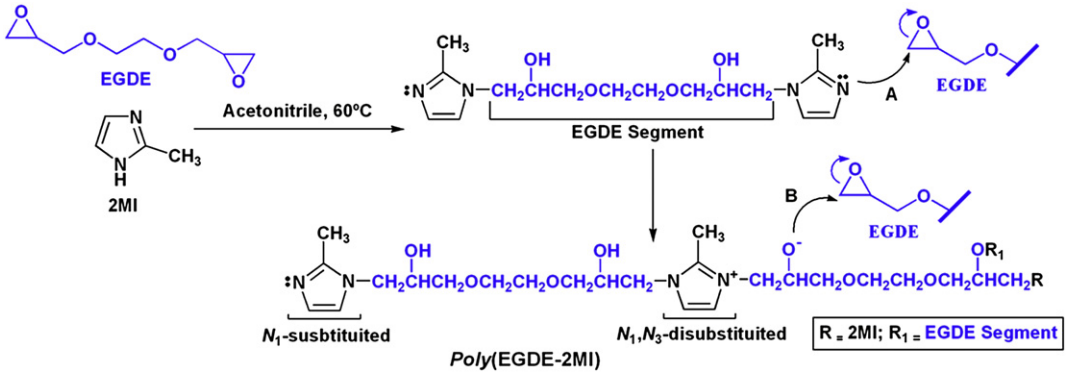

Scheme 2. Synthesis of *Poly*(EGDE-2MI).

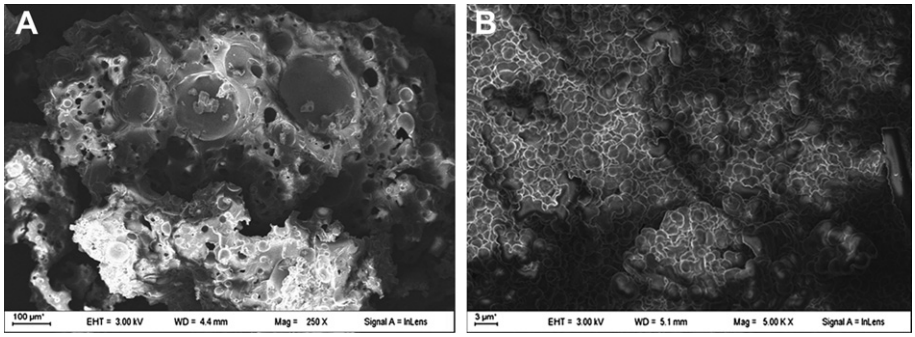

Fig. 1. SEM images for *Poly*(EGDE-2MI) (A) and *Poly*(EGDE-MAA-TRZ) (B).

regular in contrast with the surface of *Poly*(EGDE-2MI). The latter was a soft resin that cannot be milled as powdered particles as in the case of the polyampholytes bearing EGDE, MAA and the nitrogen heterocyclic units. The surfaces in the polymers were non-porous (absence of mesopores) in agreement with the information obtained from the BET adsorption isotherms, which also indicated a low specific surface area around 0.5–1 $m^2\ g^{-1}$. The surface areas determined by adsorption of water vapor gave values of around 80–300 $m^2\ g^{-1}$. In particular, *Poly*(EGDE-MAA) presented 83 $m^2\ g^{-1}$ of water vapor surface against 243 $m^2\ g^{-1}$ presented by *Poly*(EGDE-2MI), indicating a higher density of charged and polar groups in the latter. The accurate determination of the specific surface area is not straightforward due to the high density of functional groups on the particles surface. Nitrogen could neglect polar surface sites due to its non-polar character and was not the best probe for this purpose. The water molecule can measure a more realistic specific surface area because of the interactions between the probe molecule and the polar surface sites (Table 1).

Poly(EGDE-MAA-PYR) and *Poly*(EGDE-MAA-TRZ) exhibited a particularly high surface area/D_{app} ratio. In addition, *Poly*(EGDE-MAA-PYR) particles are expected to present outstanding size-related properties such as high adsorption capacity for ions and biomolecules, with many potential applications in environmental and industrial fields.

The FT-IR spectra of *Poly*(EGDE-2MI), *Poly*(EGDE-MAA-TRZ) and *Poly*(EGDE-MAA-PYR) are shown in Fig. 2, together with those of *Poly*(EGDE-MAA-IM) reported previously [20]. The bands at 1724, 1630/1445, 1570 and 1100 cm^{-1} were attributed to the stretching vibration of C=O, C=C/N (heterocyclic rings), R-CO_2^- and C-O respectively. The bending vibrations of the triazole, pyrazole and imidazole moieties and their torsion stretching were present at around 900 and between 750–600 cm^{-1} respectively.

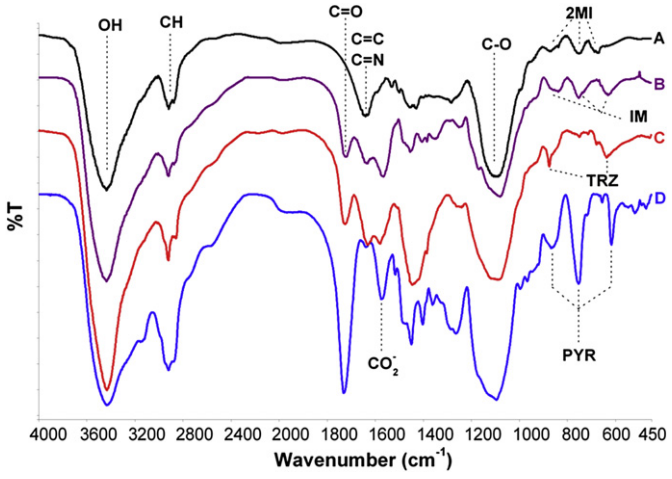

Fig. 2. FT-IR spectra of *Poly*(EGDE-2MI) (A), *Poly*(EGDE-MAA-IM) (B), *Poly*(EGDE-MAA-TRZ) (C) and *Poly*(EGDE-MAA-PYR) (D).

3.3. Solution- and solid-state NMR characterizations

The ^{13}C CP-MAS spectra of the new polyampholytes bearing triazole or pyrazole units together with the new polyelectrolyte *Poly*(EGDE-2MI) are shown in Fig. 3. Table 2 displays the corresponding chemical shifts, where the numbers of the assignments correspond to those in Fig. 3. The ^{13}C CP-MAS spectra were compared to those of *Poly*(EGDE-MAA) and *Poly*(EGDE-MAA-IM or 2MI) previously reported [27].

The new materials showed differences in the region between 110–160 ppm. In particular, the ^{13}C CP-MAS spectrum of the matrix containing pyrazole (Fig. 3E) shows that the three carbons of the heterocycle were well resolved in comparison with the materials bearing imidazole units (Fig. 3B, C and D). The ^{13}C CP-MAS spectrum for *Poly*(EGDE-2MI) showed only one type of carbon around 40-60 ppm (Fig. 3 and Table 2) in contrast with the two distinct carbon signals for the oxirane ring in reported monomers used for the synthesis of the epoxy system in solid-state NMR [28], and, in the case of our results, for the EGDE monomer presented in the Electronic Supplementary Material. In addition, the splitting observed in the correlations involving C_8 and C_{10} in the 2D ^1H-^{13}C HETCOR spectrum of *Poly*(EGDE-2MI) sensed that the imidazole moieties were in different environments (Fig. 4).

In order to clarify the assignments in these kinds of polymeric systems, solution- and solid-state experiments were performed taking into account that in all the materials the presence of C_9 was the evidence of the covalent binding between the heterocyclic ring and the EGDE segments. This C_9 was generated after the opening of the epoxy ring by the nucleophilic character of the nitrogen atom in the different heterocyclic monomers used (imidazole, triazole and pyrazole). In solid state, the problem was that the chemical shift corresponding to C_9 was, in general, very close to that of the methylene signal of the methacrylic segment (C_4) (Fig. 3).

The assignment of C_9 in reported polymeric materials containing imidazole has not been made either by omission or overlapping of different signals [20,27,29,30]. We identified the chemical shift of C_9 performing solution-state NMR experiments using a new soluble system denominated *Poly*(EGDE-IM)$_{sol}$. This material was obtained by using lower amounts of the cross-linking molecule (EGDE) and imidazole in a molar relation of 0.5:1 respectively. By comparing HSQC of EGDE and *Poly*(EGDE-IM)$_{sol}$, the chemical shift of C_9 was clearly identified (see Electronic Supplementary Material). The signal of C_9 in the ^{13}C CP-MAS spectrum of *Poly*(EGDE-2MI), where C_4 was absent, helped us to identify this resonance in the rest of the

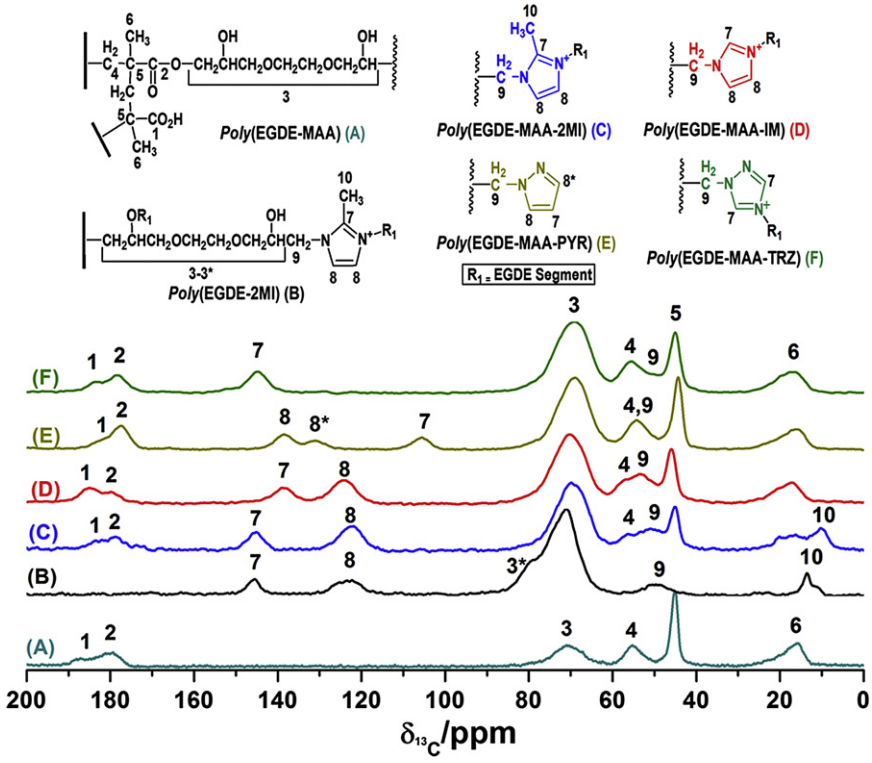

Fig. 3. ^{13}C CP-MAS spectra for *Poly*(EGDE-MAA) (A), *Poly*(EGDE-2MI) (B), *Poly*(EGDE-MAA-2MI) (C), *Poly*(EGDE-MAA-IM) (D), *Poly*(EGDE-MAA-PYR) (E) and *Poly*(EGDE-MAA-TRZ) (F).

new materials. In the case of *Poly*(EGDE-MAA-PYR or TRZ), the C_9 and C_4 chemical shifts were obtained from the deconvolution of the ^{13}C CP-MAS NMR spectrum (Fig. 5).

Note that the chemical shifts for C_9 were distinctive for each heterocyclic unit attached to it, even in the case of IM or 2MI (Table 2). The correct assignment of C_9 in the solid state was the evidence that the heterocyclic rings were attached to a non-soluble matrix through a covalent bond and not by a complexation with MAA.

3.4. Molecular mobility studied by solid-state NMR

The ^1H-^{13}C 2D-WISE NMR experiments were carried out to study the dynamics in the solid polymers. With this technique, the information about the dynamic behavior within the system can be qualitatively assessed by examining the proton linewidths associated with the different carbons in the polymer host [23]. In a previous work, we demonstrated that *Poly*(EGDE-MAA) and *Poly*(EGDE-MAA-IM) were non-homogeneous, presenting regions with different molecular mobility. This was confirmed taking into account that the ^1H projections associated with the signal at ~70 ppm (C_3) in the carbon dimension had contributions of two

Table 2
^{13}C CP-MAS chemical shifts corresponding to the polyampholytes.

δ ^{13}C (ppm)						
Polyampholytes[b]				Polyelectrolytes[c]		Carbon[a]
TRZ[b]	PYR[b]	IM[b]	2MI[b]	MAA[c]	2MI[c]	
–	–	–	12.4	–	12.2	(10)
16.8	16.7	17.1	19.6	16.0	–	(6)
45.0	44.4	45.8	46.4	45.1	–	(5)
48.9	54.2	53.2	52.5	–	49.0	(9)
55.8	54.2	57.8	56.8	55.3	–	(4)
69.1	69.2	71.3	71.0	70.9	70.1	(3)
–	–	–	–	–	78.1	(3[a])
–	131.2	–	123.6	–	–	(8[a])
–	138.6	123.7	–	–	122.0	(8)
144.8	105.7	137.8	146.3	–	144.8	(7)
178.3	177.5	180.0	180.3	179.4	–	(2)
183.7	181.9	185.0	184.4	187.2	–	(1)

[a] The assignment corresponds to those in Fig. 3.
[b] *Poly*(EGDE-MAA-TRZ or PYR or IM or 2MI).
[c] *Poly*(EGDE-MAA) and *Poly*(EGDE-2MI).

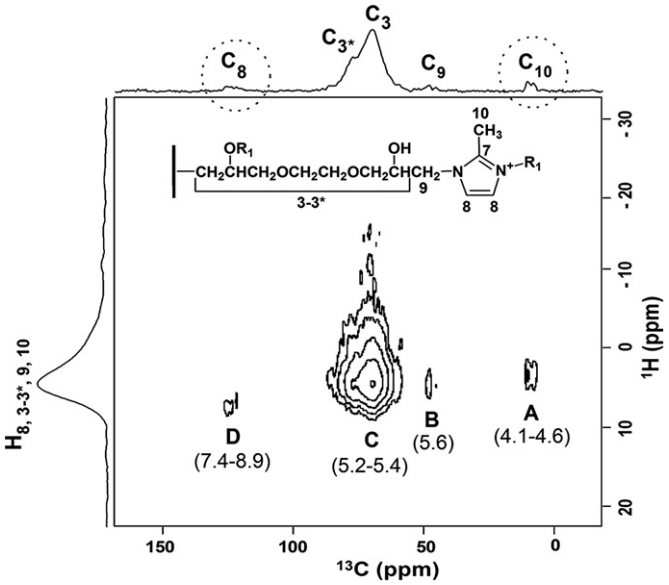

Fig. 4. ^1H-^{13}C HETCOR spectrum of *Poly*(EGDE-2MI) in the solid state. The ^1H chemical shift values (in ppm) extracted from each correlation are indicated in parenthesis. The dot-line circles show the carbon signals that present splittings.

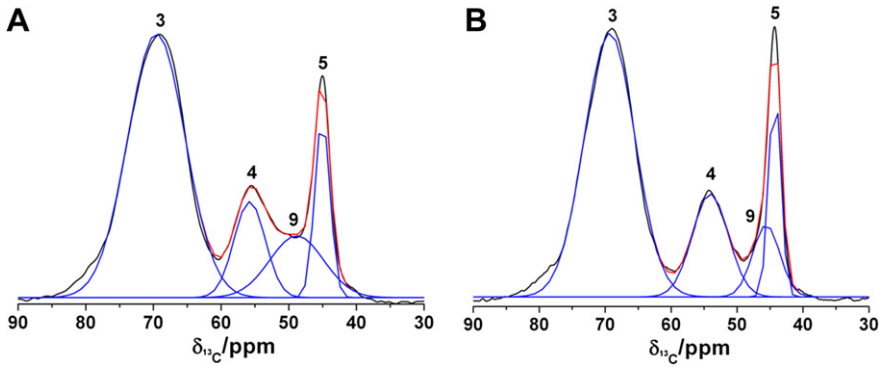

Fig. 5. Deconvolution of the ^{13}C CP-MAS spectra of *Poly*(EGDE-MAA-TRZ) (R^2: 0.9958) (A) and for *Poly*(EGDE-MAA-PYR) (R^2: 0.9963) (B), experimental data (black line), deconvolution from the experimental data (red line) and Gaussian lines from each resonance peak (blue lines). (For interpretation of the references to colour in this figure legend, the reader is referred to the web version of this article.)

lines with different widths [27]. In general, this signal is selected due to its good signal-to-noise ratio, which allows comparing between the different materials.

The high values for the full width at half height (FWHH) of the ^1H projections corresponding to C_3 in the new synthesized polyampholytes, *Poly*(EGDE-MAA-TRZ or PYR), indicate a lower molecular motion than that in *Poly*(EGDE-MAA) (Fig. 6 and Table 3). The lower mobility of the polymeric segments may arise from the interaction among the triazole or pyrazole units, which reinforced the contact among the different polymeric chains. However, the soft *Poly*(EGDE-2MI) material presented a higher FWHH than the rigid *Poly*(EGDE-MAA). In *Poly*(EGDE-MAA), the EGDE segment was more mobile than in *Poly*(EGDE-2MI). Even when the methacrylic segments are involved in the reticulation degree, the imidazole was responsible for the lower molecular mobility in a micro scale, probably resulting from the interaction between the aromatic units, but it was not enough to produce a reticulation similar to that in *Poly*(EGDE-MAA). According to these results, the EGDE segments provided mobile regions but the heterocyclic units together with the methacrylic acid were responsible for the high cross-linking degree in these polymer materials.

These results indicate that the EGDE segment was a sensitive parameter to analyze the molecular mobility in a bulk amorphous polymer when the methacrylic acid or the imidazole residues are covalently attached to this segment.

Another evidence of the low molecular motion in these systems was the measure of the proton spin-lattice relaxation time in the rotating frame ($T^H_{1\rho}$). In general, carbon magnetization in the MAA and imidazole segments in all the compounds had a single exponential decay according with Equation 1. On the other hand, the carbon magnetization in the EGDE segment (signal at ~70 ppm) followed a two-exponential behavior according with Equation 2.

$$M_C(\tau) = M_0 \times e^{-\frac{\tau}{\tau_1}} \quad (1)$$

$$\frac{M_C}{M_0}(\tau) = A \times e^{-\frac{\tau}{\tau_1}} + (1-A) \times e^{-\frac{\tau}{\tau_2}} \quad (2)$$

The decay of the magnetization of C_3 was indicative of a non-homogeneous material having regions with different mobility. Here, as the magnetization was normalized, the numbers A and 1-A, from Equations 1 and 2 can be directly interpreted as a measure of the percentage of the sample giving τ_1 and τ_2 respectively. The values of $T^H_{1\rho}$ are shown in Table 4.

The $T^H_{1\rho}$ values observed for the different carbons in each material were similar due to the spin diffusion process. The long values of the $T^H_{1\rho}$ in all the fractions of *Poly*(EGDE-MAA-TRZ or PYR) indicate that the general mobility was more affected than in the rest of the polymer materials. Fast or effective relaxations (short values for $T^H_{1\rho}$) corresponding to mobile fractions (7–13%) were detected for the EGDE segment (C_3) in both *Poly*(EGDE-MAA-TRZ) and *Poly*(EGDE-MAA-PYR), although lower than the values for *Poly*(EGDE-MAA) and *Poly*(EGDE-MAA-IM) (Table 4). These results indicate that the heterocycle units used, triazole and pyrazole, caused a decrease in the general molecular mobility, together with the reticulation induced by the MAA, explaining the high rigidity of the resulting polymers.

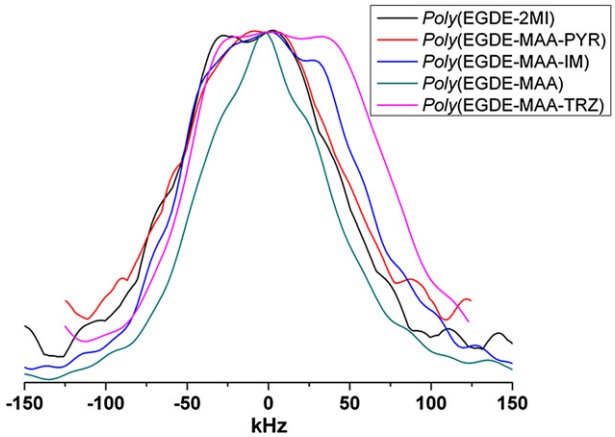

Fig. 6. ^1H projection for the C_3 extracted from the ^1H-^{13}C 2D WISE experiments in the indicated polymer materials.

3.5. Acid–base properties of the polyampholytes and polyelectrolytes

The thermodynamic data for the protonation of the heterocyclic nitrogen and the carboxylate group in the polymers were obtained and the polyelectrolyte character was explored. Each polyampholyte was placed together with a measured excess of HCl

Table 3
Full width at half height (FWHH) corresponding to the ^1H projection from the C_3 signal at 70 ppm extracted from the 2D WISE experiment in the indicated polymers.

Polymer	FWHH (kHz)
EGDE-MAA [27]	90
EGDE-2MI	120
EGDE-MAA-IM [27]	125
EGDE-MAA-PYR	124
EGDE-MAA-TRZ	140

Table 4
$T^H_{1\rho}$ (in ms) measured in the indicated polymers. The values were obtained by fitting the experimental data of ^{13}C magnetization vs. τ to Equation 1 or 2. In the case of the two-exponential decay, the fractions corresponding to the short $T^H_{1\rho}$ are displayed in parentheses.

Polymer	$T^H_{1\rho}$ (ms)							
	C_3[a]		C_4[b]	C_5[b]	C_6[b]	C_7[c]	C_8[c]	C_9[d]
EGDE-MAA [27]	3.3	0.5 (37%)	3.4	2.9	3.1	–	–	–
EGDE-MAA-IM [27]	3.3	0.6 (26%)	3.0	2.6	–	2.8	2.8	–
EGDE-MAA-PYR	5.3	0.3 (13%)	6.0	6.4	–	5.3		–
EGDE-MAA-TRZ	5.7	0.3 (7 %)	6.2	–	–	6.2		–
EGDE-2MI	2.5	0.5 (17 %)	–	–	–	2.3		2.7

[a] Carbon signals of the EGDE segments.
[b] Methacrylic segments.
[c] Heterocyclic units.
[d] The methylene from the EGDE segments attached to the heterocycle units according with the numbering in Fig. 3.

standard solution. In this condition, the polyampholyte was considered as a polymeric acid bearing two types of ionizable groups and titrated with a NaOH standard solution [31,32]. Two acid dissociation reactions can be defined for the fully protonated polymeric unit (H_2P^+):

$$H_2P^+ + H_2O \rightleftharpoons HP^\pm + H_3O^+ \quad Ka_1 = \frac{[HP^\pm] \times [H_3O^+]}{[H_2P^+]}$$

$$HP^\pm + H_2O \rightleftharpoons P^- + H_3O^+ \quad Ka_2 = \frac{[P^-] \times [H_3O^+]}{[HP^\pm]}$$

H_2P^+ represents the polymer bearing both R-CO_2H and $HetH^+$ (protonated heterocycle); $HP^\pm$ represents the neutral polymer, whereas P^- represents the polymer with R-CO_2^- and Het. Then, in order to analyze the electrostatic interaction between charged groups, the modified Henderson-Hasselbalch equation (Equations 3 and 4) can be used [33,34].

$$pH = pK^\circ + n \times \log \frac{\alpha_i}{1-\alpha_i} \quad (3)$$

$$pK = pK^\circ + (n-1) \times \log \frac{\alpha_i}{1-\alpha_i} \quad (4)$$

The empirical parameters of acidity obtained from them are shown in Table 5: α_i represents the acid dissociation degree for the carboxylic group (α MA^- = [R-CO_2^-]/$C_{total\ MAA}$) or the protonated heterocycle (α Het = [Het]/$C_{total\ Het}$), pK is the apparent acid dissociation constant for each type of acidic group, and pK° is the pK value at $\alpha_i = 0.5$. The n parameter gives a measure of the deviation of the studied polymers from the behavior of small (generally soluble) molecules showing sharp dissociation constants and $n = 1$ [35,36]. The variation of K with α is known as the polyelectrolyte effect. The magnitude of n reflects this effect and can be seen as an index of the accessibility of protons in the reversible

Table 5
Results obtained from the potentiometric titrations of the polymers.

Polymer	R-CO_2H	R-Het	pK°			
	mmol g^{-1}		R-CO_2H	n	R-$HetH^+$	n
EGDE-MAA-TRZ	0.68	1.11	6.85	1.11	4.57	1.10
EGDE-MAA-PYR	1.22	nd	6.89	1.27	nd	–
EGDE-IM	–	1.42	–	–	7.07	1.61
EGDE-MAA [20]	0.92	–	8.01	1.81	–	–
EGDE-MAA-IM [20]	1.1	1.3	4.7	1.07	7.17	1.46
EGDE-MAA-2MI [20]	1.39	1.41	4.52	1.41	7.82	1.31

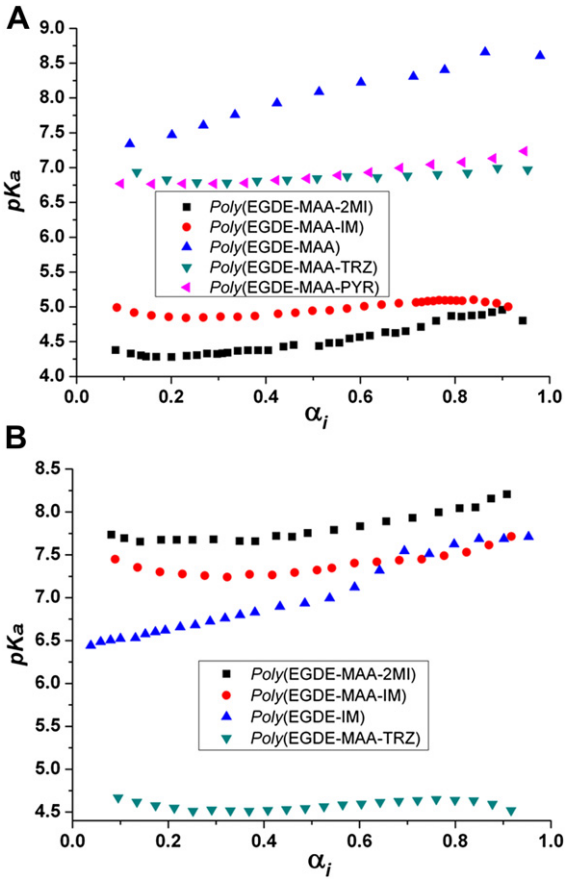

Fig. 7. pK values as a function of α_i for R-CO_2H (A) and for $HetH^+$ (B).

dissociation reaction from weak functional groups [37]. n values greater than 1 indicate that the dissociation of protons from the network becomes more difficult as α_i increases. The corresponding pK increased progressively with α_i due to a greater electrostatic field force produced by the overall negative charge density in the macromolecule.

Fig. 7 shows the results obtained from the plot of pK values as a function of α_i for the ionizable groups in the different materials for the carboxylic acid unit (Fig. 7A) or the heterocyclic unit (Fig. 7B).

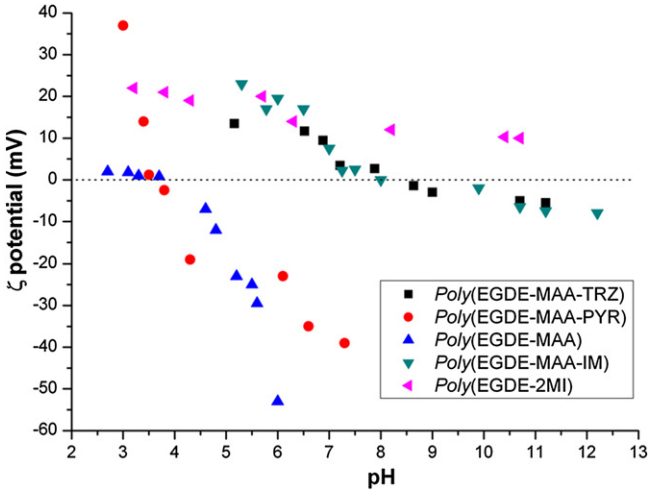

Fig. 8. Experimental zeta potential curves for the indicated materials.

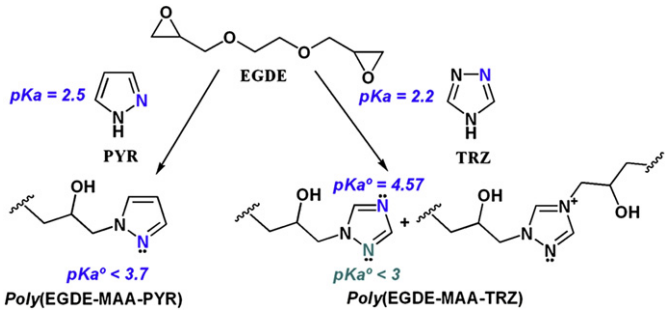

Scheme 3. Changes in the pKa values of the pyrazole and triazole residues in the polyampholytic matrixes. The methacrylic segments are not shown to clarify the analysis.

Table 5 displays the *n* values for the polyampholytes and polyelectrolytes.

For the carboxylic groups, the electrostatic attraction between H^+ and the increasing negative charges on the network would account for the increase in pK values with α_i (Fig. 7A). The effect was particularly stronger for the polyelectrolyte *Poly*(EGDE-MAA), due to a possible distribution of R-CO_2^- in clusters where the basicity was enhanced by the vicinity of groups of the same charge.

The polyelectrolyte effect was less marked in our polyampholytes than in polyelectrolytes and betaines with close neighbors of opposite charge [38]. For carboxylic residues, we found two opposite effects: on the one hand, that the high negative charge density from R-CO_2^- makes the dissociation of H^+ more difficult, and, on the other hand, that the polyampholyte presents $HetH^+$ groups and non-neutralizable positive charges from disubstituted Het residues (Het^+), which exert repulsion on the H^+ interacting with R-CO_2^- groups.

For $HetH^+$ groups, *Poly*(EGDE-IM) also presented a strong polyelectrolyte effect (Fig. 7B). In this case, the pK values were lower than those in the corresponding polyampholyte, *Poly*(EGDE-MAA-IM), attributed to the absence of negative charge.

The polyelectrolyte effect and the zeta potential values were specially low for *Poly*(EGDE-MAA-TRZ) (Fig. 8). In this material, we found the lowest amount of R-CO_2H and titrable Het groups.

Then, the pK° values were analyzed taking into account the dependence on the chemical environment surrounding each type of ionizable group (Table 5). The pK° for $HetH^+$ did not change significantly respect to the pK of the monomer, except in the case of triazole, where the pK° was more than two units higher as a consequence of the arrangement illustrated in Scheme 3. For the R-CO_2H groups, the pK° in *Poly*(EGDE-MAA-Het) was similar to the pK of MAA (4.66) when Het was IM and 2MI, but increased substantially in the polyampholytes with weak basic Het residues and in *Poly*(EGDE-MAA). These high pK° could be attributed to an increase in the cross-linking degree in the network and/or to a more hydrophobic environment [34,37,39,40].

The 2D-WISE NMR experiments (Fig. 6) and $T_{1\rho}^H$ values (Table 4) showed that the ^{1}H-^{1}H dipolar couplings in the network were smaller for *Poly*(EGDE-MAA) than for the other polymers, indicating a lower cross-linking degree for this polyelectrolyte. Then, the higher pK° in this case could be directly attributed to a more hydrophobic environment, where polar heterocycles were absent.

In the cases of *Poly*(EGDE-MAA-TRZ) and *Poly*(EGDE-MAA-PYR), the high pK° values for the R-CO_2H groups could be explained by a higher degree of cross-linking and hydrophobicity. In the first case, the unexpectedly low polyelectrolyte effect might be associated with the opposite effect of the non-neutralizable Het^+ and the negative charge of carboxylate, together with a high amount of lone R-CO_2^- spread over the side chains of the network.

In the case of *Poly*(EGDE-IM), a departure from the linearity for α higher than 0.5 can be seen for the plot of pH vs. log(α/(1-α)). This fact and the S-shaped profile in pK vs α might be associated with the presence of two types of $HetH^+$ groups (Fig. 7B) [41]. In addition, the ^{1}H-^{13}C HETCOR spectrum of *Poly*(EGDE-2MI) indicated that some imidazole moieties were in different environments, which may explain the presence of heterogeneity of the $HetH^+$ groups (Fig. 4).

3.6. Isoelectric point determination

The zeta potential values measured for the particles of polyampholytes and polyelectrolytes are depicted in Fig. 8 and Table 6.

In the case of *Poly*(EGDE-MAA), the zeta potential was zero at pH values below 4, becoming negative at pH higher than 4, as expected for a weak polyelectrolyte. *Poly*(EGDE-IM) adopted only a positive charge, giving a zeta potential of +20 mV at pH values lower than 6.5, and a zeta potential close to +10 mV at pH values between 6.5 and 11. The decrease in the zeta potential profile with an inflection at pH = 6.5 was the result of the neutralization of IMH^+, remaining positive beyond 6.5 due to the permanent charge from IM^+.

An isoelectric point (pI) for the polyampholytes can be determined using this technique. These pI values were significantly different from those obtained indirectly by potentiometric titration of the acid form of the polymers (Table 6) [18,20]. To explain this difference we must focus on the nature of the ionic and ionizable sites. These particles have carboxylate and hydroxyl groups and heterocycle residues that can be monosubstituted (Het) or disubstituted (Het^+). The Het units are weak bases that can be protonated giving $HetH^+$, and the Het^+ units bear a permanent positive electric charge. Only R-CO_2H and $HetH^+$ were determined by titration of the acid form, which leads to a theoretical pI lower than this experimental value. The amount of Het^+ was determined indirectly taking into account the pI obtained from the zeta

Table 6
Isoelectric points obtained by potentiometric titration and by zeta potential measurements, and degree of disubstitution of the Het groups obtained from these results.

Polymer	Total Het (mmol g^{-1})	Titrable Het (mmol g^{-1})	pI[a]	pI[b]	α at pI[b]	Disubstituted Het (mmol g^{-1})	Non-accessible Het (mmol g^{-1})
EGDE-MAA-TRZ	1.83	1.11 (60.5%)	5.84	8.5	1	0.68 (37%)	0.04
EGDE-MAA-PYR	1.96	nd	nd	3.7	0.01	0	nd
EGDE-IM	2.12	1.42 (67%)	–	–	–	0.26 (12%)[c]	0.44 (21%)
EGDE-2MI	2.03	1.55 (76%)	–	–	–	nd	nd
EGDE-MAA-IM	2.28	1.3 (57%)	5.8	8.0	0.90	0.86 (38%)	0.12
EGDE-MAA-2MI	2.39	1.41 (59%)	6.40	8.2	0.83	0.91 (38%)	0.07

[a] Isoelectric point obtained by potentiometric titration.
[b] Isoelectric point obtained by zeta potential.
[c] Determined by substraction of the $HetH^+$ groups (determined from titration with a NaOH standard solution) to the total of protonable Het and disubstituted Het^+OH^- groups (determined from titration with a HCl standard solution).

potential, the dissociation degree of the polymer at pH = pI [18,20], the number and type of protonated groups, and the charge balance in that situation. This estimation implied the absence of chemisorbed charged species on the surface of the particles. It was assumed that the error in this assumption was small because the charged species present in the solutions were Cl^-, Na^+ and K^+, acting predominantly as counterions of the functional groups.

For instance, at pH = pI = 8.2, the dissociation degree of *Poly*(-EGDE-MAA-2MI) was close to 0.83, with 1.39 mmol g^{-1} of R-CO_2^-, 0.93 mmol g^{-1} of 2MI and 0.48 mmol g^{-1} of $2MIH^+$. At this point, the amount of positive charge in the polymer should equal the negative charge of the carboxylate, in accordance with the measurements of zeta potential. The "missing" positive charge for neutrality (0.91 mmol g^{-1}) could only be explained by the permanent positive charges of the $2MI^+$ units. In the same way, at pH = pI = 8.0, the dissociation degree of *Poly*(EGDE-MAA-IM) was 0.90 with 1.1 mmol g^{-1} of R-CO_2^-, 1.06 mmol g^{-1} of IM and 0.24 mmol g^{-1} of IMH^+. In this case, the "missing" positive charge for neutrality (0.86 mmol g^{-1}) could be explained by the permanent positive charges of the IM^+ units.

The total number of heterocycle residues in the polymers deduced from the elemental analysis was compared with the number of titrable Het and of Het^+. From this analysis, we observed that a certain number of residues was not detected ("non accessible Het").

For *Poly*(EGDE-MAA-TRZ), the $TRZH^+$ group was more acidic than R-CO_2H. *Poly*(EGDE-MAA-TRZ) exhibited zero charge at pH = 8.5, and the dissociation degree was 1.0. Again, the presence of positive charges at a pH much higher than the pKa° of R-CO_2H (6.85) was due to the disubstitution of the units of heterocycles. At pH values higher than 8.5, the zeta potential values were close to zero because the number of TRZ^+ units was similar to that of R-CO_2^- (0.68 mmol g^{-1}) (Fig. 8).

For *Poly*(EGDE-MAA-IM), the zeta potential profile at pH values higher than pI was also close to zero because the maximal negative net charge was relatively small (0.24 mmol g^{-1}).

For *Poly*(EGDE-MAA-PYR), the $PYRH^+$ group was expected to be more acidic than R-CO_2H. Its pI was 3.7, significantly lower than that for the other polyampholytes, and the profile of zeta potential was very similar to that of *Poly*(EGDE-MAA), which is a polyelectrolyte bearing R-CO_2^- groups. These features, analyzed together with the number of carboxyl groups and the amount of nitrogen found from the elemental analysis, suggest the absence of disubstitution and the absence of permanent positive charges.

The lack of permanent positive charges associated with the presence of heterocycles is the probable cause of a significantly low D_{app} for *Poly*(EGDE-MAA-PYR) particles. This outstanding feature will be object of further research to clarify the relationship and to handle the particle size.

In summary, the N_1,N_3-disubstitution in triazole units created a permanent positive charge which affected the resulting zero charge point. The evolution to a N_1,N_2-disubstituted pyrazole ring was less probable, because the reaction of a N_1-substituted pyrazole unit with an epoxy ring would generate a positive permanent charge adjacent to a nitrogen atom. In contrast, the 1*H*-1,2,4-triazole has one pyrrolic type nitrogen (N_1) and two pyridinic-type nitrogen atoms ($N_{2,4}$), one of which is similar to the pyrazole (N_2) and the other which is similar to the imidazole ring (N_4). Therefore, the N_1-substituted triazole has two potential nitrogen atoms to react with another EGDE molecule, being more likely to occur through the N_4 than through the N_2, as described in the case of pyrazole.

3.7. Swelling degree of the polymers

The water content of polyampholytes and polyelectrolytes is related to charge solvation. The repulsive forces among fixed charges and the osmotic pressure due to counterions induce network expansion [42,43]. The results for these new materials are summarized in Table 7. First, the ionic strength of the solution in contact with the polymers was varied at pH = 3.0. As expected, in all the materials ionized at pH = 3.0, there was a decrease in water content upon addition of salt. At a low ionic strength, the osmotic pressure in the external solution was lower than that in the inner solution in contact with the ionized groups of the network. The solvation of these charges and their counterions induced the swelling of the polymer. When the ionic strength of the external solution was increased, the difference in osmotic pressure was lower and the salt of low molecular weight screened the network charged electrostatically, forcing the polymer to shrink. Then, the ionic strength was kept constant with NaCl at pH = 3.0 and 9.8 to study the effect of pH on the swelling degree.

Table 7
Equilibrium swelling and water content of the polymers. Dependence on pH and ionic strength (I).

Polymer	pH 3.0 I < 0.001		pH 3.0 I = 0.5		pH 9.8 I = 0.5	
	Swelling (g g^{-1})	Water content (%)	Swelling (g g^{-1})	Water content (%)	Swelling (g g^{-1})	Water content (%)
EGDE-MAA	1.09	52	1.05	51	1.50	60
EGDE-2MI	3.10	76	2.21	69	1.92	66
EGDE-MAA-IM	4.90	83	3.20	76	3.60	78
EGDE-MAA-2MI	5.30	84	4.60	82	4.20	81
EGDE-MAA-PYR	2.80	74	2.17	68	3.09	76
EGDE-MAA-TRZ	3.55	78	2.53	72	3.05	75

In the polyelectrolytes, the swelling followed a profile similar to that of the zeta potential. For *Poly*(EGDE-MAA), the swelling was minimal at pH = 3.0, not affected by the ionic strength because R-CO_2H was not dissociated, and the water content increased at pH = 9.8. In *Poly*(EGDE-2MI), the swelling was low at pH = 9.8 and slightly increased at pH = 3.0, where the 2MI units were protonated. Comparing both polyelectrolytes, it can be observed that the second one exhibited a higher swelling degree and water content, associated with a more polar environment given by 2MI, $2MIH^+$ and $2MI^+$.

The polyampholytes swelled both in acidic and alkaline conditions. The higher water content of *Poly*(EGDE-MAA-IM) and *Poly*(-EGDE-MAA-2MI) was due to the higher number of total ionic and ionizable functional groups. In *Poly*(EGDE-MAA-PYR) (pI = 3.7), the water content and swelling degree were higher at pH = 9.8 than at pH = 3.0. Here we must take into account the absence of permanent positive charges from the heterocycle, and the absence of negative charge at pH = 3.0. For *Poly*(EGDE-MAA-TRZ) (pI = 8.5), the water content was slightly higher at pH = 9.8, even if there were more ionized groups at acid pH.

4. Conclusions

Polyampholytes and polyelectrolytes bearing *N*-heterocycles, ethylene glycol diglycidyl ether and/or methacrylic acid were successfully synthesized in a simple one-spot strategy.

NMR experiments in the solid state (^{13}C CP-MAS and ^1H-^{13}C HETCOR), together with experiments in the solution state (HSQC), were crucial to confirm the covalent binding of the heterocyclic ring to the polymer backbone through the nitrogen atom. In particular, the signal around 50 ppm was unambiguously assigned to C_9 in the spectra of the materials containing imidazole, 2-methylimidazole, triazole and pyrazole.

2D-WISE NMR experiments, together with the $T^{H}_{1\rho}$ experiments, gave relevant information about the proton network and the dynamic behavior of the polymers.

The higher synthetic yield was correlated with a lower molecular motion and a higher cross-linking degree for the polyampholytes bearing triazole or pyrazole, associated with the lower tendency of these monomers to form ionic pairs with methacrylic acid.

We carried out a comprehensive study of the properties of polyelectrolytes and polyampholytes in the different polymeric materials synthesized. Zeta potential measurements allowed determining the isoelectric point in the polyampholytes. On the other hand, the results of potentiometric titrations brought qualitative and quantitative information on the weak acid and basic residues. Finally, the simultaneous analysis of these two features allowed us to assess the degree of disubstitution of the heterocyclic residues in these materials. The quaternization of imidazole and triazole residues was confirmed.

Our synthetic strategy leads to the production of non-soluble functionalized polymers. The outstanding adsorption capacity for polar species related to the high density of binding sites makes these materials attractive for analytical, environmental and biotechnological processes.

Acknowledgments

The authors thank the financial support from Universidad de Buenos Aires (UBACyT 10-12/237 and 109), Universidad Nacional de Córdoba (SECyT-UNC 05/B436), CONICET (CONICET 2010-2012/PIP 076 and 441), ANPCyT (BID 1728/PICT 01778). J.M. Lázaro Martínez thanks the CONICET for his postdoctoral fellowships.

Appendix. Supplementary material

Supplementary data related to this article can be found online at doi:10.1016/j.polymer.2012.01.031.

References

[1] Lowe AB, McCormick CL. Chem Rev 2002;102:4177–89.
[2] Ciferri A, Kudaibergenov SE. Macromol Rapid Commun 2007;28:1953–68.
[3] Braun O, Selb J, Candau F. Polymer 2001;42:8499–510.
[4] Colak S, Tew GN. Macromolecules 2008;41:8436–40.
[5] Munk P. In: Munk P, Aminabhavi TM, editors. Introduction to macromolecular science. 2nd ed. New York: Wiley-Interscience; 2002. p. 56–8.
[6] van Berkel PM, Punt M, Koolhaas GJAA, Driessen WL, Reedijk J, Sherrington DC. React Funct Polym 1997;32:139–51.
[7] Hadjikallis G, Hadjiyannakou SC, Vamvakaki M, Patrickios CS. Polymer 2002; 43:7269–73.
[8] Hawkins D, Stevenson D, Reddy S. Anal Chim Acta 2005;542:61–5.
[9] Lázaro Martínez JM, Leal Denis MF, Denaday LR, Campo Dall' Orto V. Talanta 2009;80:789–96.
[10] Neyret S, Ouali L, Candau F, Pefferkorn E. J Colloid Interface Sci 1995;176: 86–94.
[11] Wu CF, Chen WY, Lee JF. J Colloid Interface Sci 1996;183:236–42.
[12] Patel RN, Singh N, Shukla KK, Chauhan UK. Spectrochim Acta, Part A 2005;61: 287–97.
[13] Kronina VV, Wirth HJ, Hearn MTW. J Chromatogr, A 1999;852:261–72.
[14] (a) Yasuda T, Namekawa K, Iijima T, Yamamoto T. Polymer 2007;48:4375–84; (b) Chen SH, Shiau CS, Tsai LR, Chen Y. Polymer 2006;47:8436–43; (c) Anderson EB, Long TE. Polymer 2010;51:2447–54.
[15] Bohmer R, Heesterbeek WHA, Deratani A, Renard E. Colloids Surf, A 1995;99: 53–64.
[16] Kumar A, Lahiri SS, Singh H. Int J Pharm 2006;323:117–24.
[17] Shiomi T, Matsui M, Mizukami F, Sakaguchi K. Biomaterials 2005;26:5564–71.
[18] Leal Denis MF, Carballo RR, Spiaggi A, Dabas P, Campo Dall' Orto V, Lázaro Martínez JM, Buldain GY. React Funct Polym 2008;68:169–81.
[19] Lázaro Martínez JM, Leal Denis MF, Piehl LL, Rubín de Celis E, Buldain GY, Campo Dall' Orto V. Appl Catal, B 2008;82:273–83.
[20] Lázaro Martínez JM, Leal Denis MF, Campo Dall' Orto V, Buldain GY. Eur Polym J 2008;44:392–407.
[21] Bennet AE, Rienstra CM, Auger M, Lakshmi KV, Griffin RG. J Chem Phys 1995; 103:6951–8.
[22] Fung BM, Khitrin AK, Ermolaev K. J Magn Reson 2000;142:97–101.
[23] Schmidt-Rohr K, Clauss J, Spiess HW. Macromolecules 1992;25:3273–7.
[24] van Rossum BJ, Förster H, de Groot HJM. J Magn Reson 1997;124:516–9.
[25] Barton JM, Hamerton I, Howlin BJ, Jones JR, Liu S. Polymer 1998;39:1929–37.
[26] Chen YC, Chiu WY, Lin KF. J Polym Sci, Part A: Polym Chem 1999;37:3233–42.
[27] Lázaro Martínez JM, Chattah AK, Monti GA, Leal Denis MF, Buldain GY, Campo Dall' Orto V. Polymer 2008;49:5482–9.
[28] Brus J, Spirkova M, Hlavata D, Strachota A. Macromolecules 2004;37:1346–57.
[29] Chiu YS, Wu KH, Chang TC. Eur Polym J 2003;39:2253–9.
[30] van Berkel PM, Driessen WL, Reedijk J, Sherrington DC, Zitsmanis A. React Funct Polym 1995;27:15–28.
[31] Annenkov VV, Danilovtseva EN, Tenhu H, Aseyev V, Hirvonen SP, Mikhaleva AI. Eur Polym J 2004;40:1027–32.
[32] Annenkov VV, Danilovtseva EN, Saraev VV, Mikhaleva AI. J Polym Sci, Part A: Polym Chem 2003;41:2256–63.
[33] Casolaro M, Bottari S, Cappelli A, Mendichi R, Ito Y. Biomacromolecules 2004; 5:1325–32.
[34] Soldatov VS. React Funct Polym 1998;38:73–112.
[35] Merle Y. J Phys Chem 1987;91:3092–8.
[36] Patrickios CS. J Colloid Interface Sci 1995;175:256–60.
[37] Ali SA, Al-Muallem HA, Wazeer MIM. J Polym Sci, Part A: Polym Chem 2002; 40:2464–77.
[38] Racovita S, Vasiliu S, Neagu V. Iran Polym J 2010;19:333–41.
[39] Philippova OE, Hourdet D, Audebert R, Khokhlov AR. Macromolecules 1997; 30:8278–85.
[40] Michaeli I, Katchalsky A. J Polym Sci 1957;23:683–96.
[41] Porasso RD, Benegas JC, van den Hoop MAGT, Paoletti S. Biophys Chem 2000; 86:59–69.
[42] Kokufuta E. Langmuir 2005;21:10004–15.
[43] Guo X, Ballauff M. Phys Rev E 2001;64:051406.